Available online at www.sciencedirect.com
ScienceDirect
Journal of Sound and Vibration 301 (2007) 189–206
JOURNAL OF SOUND AND VIBRATION
www.elsevier.com/locate/jsvi

Further investigations on Rayleigh waves in piezothermoelastic materials

J.N. Sharma*, Vishal Walia

Department of Applied Sciences, National Institute of Technology, Hamirpur, HP 177005, India

Received 23 January 2006; received in revised form 19 September 2006; accepted 25 September 2006
Available online 7 November 2006

Abstract

The present paper is devoted to extend the study on propagation of Rayleigh surface waves in homogeneous, transversely isotropic, piezothermoelastic semi-space subjected to stress free, open or closed circuit, thermally insulated/isothermal boundary conditions, in the context of non-classical (generalized) theories of thermoelasticity. Secular equations for surface wave propagation in the considered media are derived from a coupled system of governing partial differential equations of linear generalized piezothermoelasticity. The surface amplitudes, specific loss factor, and surface particle motion are also investigated. The surface particle paths during the motion are found to be elliptical which degenerate into straight lines in case there is no phase difference between horizontal and vertical components of surface displacements. The results in the context of coupled theory of thermoelasticity can be obtained from the present analysis by setting thermal relaxation parameters equal to zero. Finally, in order to illustrate and verify the analytical developments, the numerical solution of secular equations, specific loss factor, eccentricities, and inclination of particle paths with wave normal is carried out for cadmium-selenide (6 mm class) material with the help of Descartes' algorithm and functional iteration method. The computer simulated results are then presented graphically in order to illustrate and compare them in the context of coupled and generalized theories of thermoelasticity.

1. Introduction

In 1880, Curie and Curie [1] discovered an unusual characteristic of certain crystalline minerals. These materials become electrically polarized on the application of mechanical force. The Curie brothers discovered the direct piezoelectric effect that a crystal of sufficiently low symmetry develops an electric polarization under the influence of an external mechanical force, the magnitude of which is linearly proportional to the stress. About 1 year later the inverse effect, i.e. deformation of a crystal experiences an electric field was predicted. The authors [2–6] gave further foundation to various concepts and applications of piezoelectric and electromagnetic solids. The thermo-piezoelectricity theory was first proposed by Mindlin [7], who later on derived the governing equations of a thermo-piezoelectric plate [8]. The physical laws for the thermo-piezoelectric materials have been explored by Nowacki [9–11]. Chandrasekhariah [12,13] developed the

*Corresponding author. Tel.: +91 1972 254122; fax: 91 1972 223834.
E-mail address: jns@recham.ernet.in (J.N. Sharma).

0022-460X/$ - see front matter © 2006 Elsevier Ltd. All rights reserved.
doi:10.1016/j.jsv.2006.09.018

generalized theory of thermo-piezoelectricity by taking into account the finite speed of propagation of thermal disturbances. Several studies related to the propagation of waves in plates, cylinders and general three-dimensional thermo-piezoelectric material bodies, have been carried out by the investigators [14–20]. Yang and Batra [21] studied the effect of heat conduction on shift in the frequencies of a freely vibrating linear piezoelectric body with the help perturbation methods. During the past three decades, non-classical theories [22,23] have been developed to remove the paradox of infinite velocity of heat transportation. These non-classical theories of thermoelasticity have also been experimentally evidenced. Sharma and Kumar [24] have studied the propagation of plane harmonic waves in anisotropic piezo-thermoelastic materials. Sharma and Pal [25] and Sharma et al. [26] studied the propagation of Lamb waves in transversely isotropic piezothermoelastic plates subjected to (i) charge and stress free, thermally insulated or isothermal boundary conditions and (ii) stress free, electrically shorted, thermally insulated or isothermal surface conditions, in the context of coupled theory of piezothermoelasticity respectively. Sharma et al. [27] investigated the propagation characteristics of Rayleigh waves in transversely isotropic piezothermoelastic material half space in the context of conventional coupled thermoelasticity. Sharma et al. [28] presented the free vibration analysis of a homogeneous, transversely isotropic, piezothermoelastic cylindrical panel based on three dimensional piezoelectric thermoelasticity. Sharma and Walia [29] investigate the propagation of straight and circular crested waves in generalized piezothermoelastic materials. No systematic study, analytically or computational, on the propagation of Rayleigh waves in piezothermoelastic materials in the context of nonclassical (generalized) theories of thermoelasticity is available in the literature as per the knowledge of the authors. According to Achenbach [30], unlike the hyperbolic solution, the classical solution shows no distinct wave front and temperature increase starts at the initial time as expected. However, the difference in the predicted temperature between the two theories is small and only apparent for very small time scales (on the order of 100 ps). In the case of NDE applications, we are typically interested in time scales on the order of microseconds. These time scales are large enough for the solution given by both the theories to be numerically undistinguishable. Consequently, the selection of the theory for the time scales of interest can be done for convenience with no practical effect on calculated results. Likewise, the choice of a specific value for the heat propagation speed in the hyperbolic equation does not affect the results. However, from the practical point of view, the choice of a value for a heat propagation speed equal to the speed of longitudinal waves in the hyperbolic formulation, presents some numerical advantages. Keeping all this in mind the hyperbolic model of governing equations has been used to study the instant problem.

An attempt has been made to extend the analysis of Sharma et al. [27], in order to investigate the effect of relaxation time on the propagation and other characteristics of Rayleigh surface waves in homogeneous, transversely isotropic, generalized piezothermoelastic half space subjected to stress free, thermally insulated/isothermal and charge free (open circuit) or electrically shorted (closed circuit) boundary condition in the present paper. The Rayleigh dispersion relations have been obtained in both the cases of wave propagation in the half space. The amplitudes of surface displacements, electric potential and temperature change are computed in addition to the surface particle paths exploration. The phase velocity, attenuation coefficient and specific loss of energy have also been computed. Finally, the numerical solution of various secular equations and other relevant relations is carried out for cadmium-selenide (6 mm class) material in order to compare and illustrate the analytical developments.

2. Formulation of the problem

We consider a homogeneous, transversely isotropic, generalized piezothermoelastic half space initially at uniform temperature T_0 and electric potential ϕ_0. We take origin of the co-ordinate system (x, y, z) at any point on the plane horizontal surface. We take z-axis along the axis of material symmetry (elastic and thermal) and pointing vertically downward into the half space, which is thus represented by $z \geqslant 0$. The poling axis of the piezoelectric material is also assumed to coincide with z-axis. The surface $z = 0$ is subjected to stress free, thermally insulated or isothermal and charge free (open circuit) or electrically shorted (closed circuit) boundary conditions. We chose x-axis in the direction of wave propagation so that all particles on a line parallel to y-axis are equally displaced. Therefore, all the field quantities will be independent of y coordinate. Further, the disturbance is assumed to be confined to the neighborhood of the free surface $z = 0$ and hence

vanishes as $z \to \infty$. Let $\vec{u}(x,z,t) = (u,0,w)$ be the displacement vector, $\phi(x,z,t)$ is the electric potential and $T(x,z,t)$ denotes temperature change in the medium. The non-dimensional basic governing Eqs. [29] for homogeneous, transversely isotopic, linear generalized piezothermoelasticity; in the absence of charge density; heat sources and body forces, are given by [29],

$$u_{,xx} + c_2 u_{,zz} + c_3 w_{,xz} + \in_p e_1 \phi_{,xz} - (T + t_1 \delta_{2k} \dot{T})_{,x} = \ddot{u}, \tag{1}$$

$$c_3 u_{,xz} + c_2 w_{,xx} + c_1 w_{,zz} + \in_p (e_2 \phi_{,xx} + \phi_{,zz}) - \bar{\beta}(T + t_1 \delta_{2k} \dot{T})_{,z} = \ddot{w} \tag{2}$$

$$e_1 u_{,xz} + e_2 w_{,xx} + w_{,zz} - \eta_3 \in_p (\bar{\in} \phi_{,xx} + \phi_{,zz}) + p(T + t_1 \delta_{2k} \dot{T})_{,z} = 0 \tag{3}$$

$$T_{,xx} + \bar{K} T_{,zz} - (\dot{T} + t_0 \delta_{1k} \ddot{T}) = \in \left(\frac{\partial}{\partial t} + t_0 \delta_{1k} \frac{\partial^2}{\partial t^2} \right) [u_{,x} + \bar{\beta} w_{,z} - \in_p p \phi_{,z}]. \tag{4}$$

The above system of coupled partial differential equations is also subjected to the following non-dimensional boundary conditions at the surface $z = 0$ of half space are given by

(a) *Stress free surface:*

$$\sigma_{zz} = 0, \sigma_{xz} = 0. \tag{5.1}$$

(b) *Thermal boundary conditions:*

For thermally insulated (or isothermal) surface of the half space, we have

$$T_{,z} = 0 \quad (\text{or } T = 0). \tag{5.2}$$

(c) *Charge- free (open circuit) surface:*

$$D_z = 0. \tag{5.3}$$

(d) *Electrically shorted (closed circuit) surface:*

$$\phi = 0. \tag{5.4}$$

where D_z and ϕ are, respectively, the electrical displacement and electric potential.

Here, we have defined the following quantities (primes have been suppressed for convinience)

$$\begin{aligned}
&x' = \frac{\omega^* x}{v_P},\ z' = \frac{\omega^* z}{v_p},\ t' = \omega^* t,\ u' = \frac{\rho \omega^* v_p u}{\beta_1 T_0},\ w' = \frac{\rho \omega^* v_p w}{\beta_1 T_0},\ T' = \frac{T}{T_0},\ \phi' = \frac{\phi}{\phi_0},\\
&\omega^* = \frac{C_e c_{11}}{K_{11}},\ \in = \frac{T_0 \beta_1^2}{\rho C_e c_{11}},\ \sigma'_{ij} = \frac{\sigma_{ij}}{\beta_1 T_0},\ \bar{\beta} = \frac{\beta_3}{\beta_1},\ \bar{K} = \frac{K_{33}}{K_{11}},\ v_P = \sqrt{\frac{c_{11}}{\rho}} p = \frac{p_3 c_{11}}{\beta_1 e_{33}},\\
&c_1 = \frac{c_{33}}{c_{11}},\ c_2 = \frac{c_{44}}{c_{11}},\ c_3 = \frac{c_{13} + c_{44}}{c_{11}},\ c_4 = \frac{c_{11} - c_{12}}{2c_{11}},\ t'_0 = t_0 \omega^*,\ t'_1 = t_1 \omega^*\\
&e_2 = \frac{e_{15}}{e_{33}},\ \bar{\in} = \frac{\in_{11}}{\in_{33}},\ \in_P = \frac{\omega * e_{33} \phi_0}{v_P \beta_1 T_0},\ \eta_3 = \frac{\in_{33} c_{11}}{e_{33}^2},\ e_1 = \frac{e_{15} + e_{31}}{e_{33}},\\
&\beta_1 = (c_{11} + c_{12})\alpha_1 + c_{13}\alpha_3,\ \beta_3 = 2c_{13}\alpha_1 + c_{33}\alpha_3.
\end{aligned} \tag{6}$$

where ε is the thermo-elastic coupling constant, ω^* is the characteristic frequency of the medium, $\in_p$ is the piezothermoelastic coupling constant and v_P is the longitudinal wave velocity in the medium. The primes have been suppressed for convenience. α_1, K_{11} are coefficients of linear thermal expansion and thermal conductivity respectively, in the direction orthogonal to axes of symmetry, α_3, K_3 the corresponding quantities along the axis of symmetry; ρ, C_e are respectively, the density and specific heat at constant strain, c_{ij} are the isothermal elastic parameters, e_{ij} are the piezoelectric constants, $\in_{11}$ and $\in_{33}$ are electric permittivity perpendicular and

along the axis of symmetry, t_0, t_1 are thermal relaxation times and p_3 is pyroelectric constant. Here the superposed dot denotes time differentiation and coma notation is used for spatial derivatives. The symbol δ_{1k} is the Kronecker's delta in which $k=1$ corresponds to Lord–Shulman (LS) and $k=2$ refers to Green–Lindsay theory of thermoelasticity.

3. Solution of the problem and secular equations

We assume solution of the form

$$(u, w, \phi, T) = (1, V, W, S)\, U \exp[\mathrm{i}\xi(x \sin\theta + m z - ct)], \tag{7}$$

where $\xi(\xi' = (\xi v_P/\omega^*)$, $\omega(\omega' = (\omega/\omega^*))$and $c(c'/c_1)$are, respectively, the non-dimensional wave number, angular frequency and phase velocity of the wave with suppressed prime. The quantities are related with each other through the relation $c = (\omega/\xi)$. Here θ is the angle of inclination of wave normal with axes of symmetry (z-axis), m is still an unknown parameter which signifies the penetration depth of the waves; V, W and S are, respectively the amplitude ratios of displacement w, electric potential ϕ and temperature change T to that of displacement u. The use of solutions (7) in Eqs. (1)–(4) leads to a system of four coupled equations in terms of amplitudes $[1, V, W, S]^{\mathrm{T}}$. This provides us a nontrivial solution if the determinant of the coefficients of $[1, V, W, S]^{\mathrm{T}}$ vanishes. This requirement leads to following polynomial characteristic equations

$$\begin{aligned} m^8 &+ \left(a_1 + \frac{s^2}{\bar{K}} - \frac{\tau_0 F c^2}{\bar{K}}\right) m^6 + \left(a_2 + a_1 \frac{s^2}{\bar{K}} - \frac{\tau_0 F c^2}{\bar{K}} A_1\right) m^4 \\ &+ \left(a_3 + a_2 \frac{s^2}{\bar{K}} - \frac{\tau_0 F c^2}{\bar{K}} A_2\right) m^2 + \left(a_3 \frac{s^2}{\bar{K}} - \frac{\tau_0 F c^2}{\bar{K}} A_3\right) = 0 \end{aligned} \tag{8}$$

where $s = \sin\theta$, and the coefficients F, τ_0, a_i and A_i, $i = 1,2,3$ are defined in Appendix. Eq. (8) being a biquadratic in m^2 provides us eight characteristics values for m. Observing that we are interested in surface waves only, the characteristic roots m_i must satisfy the radiation condition $\mathrm{Im}(m_i) \geqslant 0$ so that motion is confined to the free surface of the half space. For each m_q, $q = 1, 2, 3, 4$, the amplitude ratios V, W, and S can be expressed as

$$V_q = \Delta_1(m_q)/\Delta(m_q),\ W_q = \Delta_2(m_q)/\Delta(m_q),\ S_q = \Delta_3(m_q)/\Delta(m_q) \tag{9}$$

where $\Delta(m_q)$ and $\Delta_i(m_q)$, $i = 1, 2, 3$, are given in Appendix.

Combining Eqs. (9) with constitutive relations given below

$$\begin{aligned} \sigma_{zz} &= (c_3 - c_2)u_{,x} + c_1 w_{,z} + \in_P \phi_{,z} - \bar{\beta}(T + t_1 \delta_{1k}\, \dot{T}) \\ \sigma_{xz} &= c_2(u_{,z} + w_{,x}) + \in_P e_2 \phi_{,x} \\ D_z &= (e_1 - e_2)u_{,x} + w_{,z} - \in_\eta \phi_{,z} + p(T + t_1 \delta_{1k}\, \dot{T}) \end{aligned} \tag{10}$$

we rewrite the formal bounded solution for displacements, temperature and electric potential, as

$$(u, w, \phi, T) = \sum_{q=1}^{4} (1, V_q, W_q, S_q) U_q \exp\left[\mathrm{i}\xi(x \sin\theta + m_q z - ct)\right]. \tag{11}$$

The stresses, electric displacement and temperature gradient, are obtained as

$$(\sigma_{zz}, \sigma_{xz}, D_z, T_{,z}) = \sum_{r=1}^{4} \mathrm{i}\xi (D_{1r}, D_{2r}, D_{3r}, m_r S_r) U_r \exp[\mathrm{i}\xi(x \sin\theta + m_r z - ct)], \tag{12}$$

where

$$D_{1r} = (c_3 - c_2) \sin\theta + c_1 m_r V_r + \in_p m_r W_r + \bar{\beta}\tau_1 c S_r, \tag{13.1}$$

$$D_{2r} = c_2 m_r + c_2 \sin\theta V_r + \in_p e_2 \sin\theta W_r, \tag{13.2}$$

$$D_{3r} = (e_1 - e_2)\sin\theta + m_r V_r - \epsilon_\eta m_r W_r - p\tau_1 c S_r,\ r = 1,2,3,4, \tag{13.3}$$

and τ_1 is defined by eq (A.4c) in Appendix.

Now we shall derive secular equations of Rayleigh waves by considering four situations depending upon different sets of boundary conditions. Upon invoking boundary conditions (5) at the surface $z = 0$, we obtain homogeneous systems of four simultaneous linear equations in amplitudes U_r, $r = 1,2,3,4$, in each case which have a nontrivial solution if and only if the determinants of their coefficients vanish. After applying lengthy algebraic reductions and manipulations, these systems lead to the following secular equations for the propagation of modified guided waves in stress-free piezothermoelastic half space under different situations and conditions. We have

$$S_1 G_1 - S_2 G_2 + S_3 G_3 - S_4 G_4 = 0, \tag{14}$$

$$S_1 G_1' - S_2 G_2' + S_3 G_3' - S_4 G_4' = 0 \tag{15}$$

for isothermal ($h \to \infty$), open and closed circuit, surface of the half space, respectively. Also

$$m_1 S_1 G_1 - m_2 S_2 G_2 + m_3 S_3 G_3 - m_4 S_4 G_4 = 0, \tag{16}$$

$$m_1 S_1 G_1' - m_2 S_2 G_2' + m_3 S_3 G_3' - m_4 S_4 G_4' = 0 \tag{17}$$

for thermally insulated ($h \to 0$), open and closed circuit, surface of the half space, respectively. Here

$$\begin{aligned}
G_1 &= D_{12}(D_{23}D_{34} - D_{33}D_{24}) - D_{13}(D_{22}D_{34} - D_{32}D_{24}) + D_{14}(D_{22}D_{33} - D_{32}D_{23}),\\
G_2 &= D_{11}(D_{23}D_{34} - D_{24}D_{33}) - D_{13}(D_{21}D_{34} - D_{31}D_{24}) + D_{14}(D_{21}D_{33} - D_{31}D_{23}),\\
G_3 &= D_{11}(D_{22}D_{34} - D_{24}D_{32}) - D_{12}(D_{21}D_{34} - D_{31}D_{24}) + D_{14}(D_{21}D_{32} - D_{31}D_{22}),\\
G_4 &= D_{11}(D_{22}D_{33} - D_{23}D_{32}) - D_{12}(D_{21}D_{33} - D_{31}D_{23}) + D_{13}(D_{21}D_{32} - D_{31}D_{22}),
\end{aligned} \tag{18}$$

where D_{1r}, D_{2r} and D_{3r} are defined in Eqs. (13) and G_i', $i = 1,2,3,4$ are written from G_i, $i = 1,2,3,4$ defined in Eqs. (18) by replacing D_{3r} with W_r, $r = 1,2,3,4$.

Eqs. (14)–(17) are Rayleigh surface wave secular equations for charge free electrically shorted, isothermal and charge-free electrically shorted, thermally insulated boundaries of piezothermoelastic half space, respectively. These secular equations contain complete information about the phase velocity, wave number and attenuation coefficient of the Rayleigh waves in such media. In general, wave number and hence the phase velocity of the waves is complex quantity, therefore the waves are attenuated in space. In the absence of thermal relaxation effect ($t_1 = t_0 = 0$) the above analysis reduces to that of Sharma et al. [27] in case of coupled piezothermoelasticity. The result in special cases of piezoelectricity, coupled piezothermoelasticity, coupled thermoelasticity and stress-free elastic plate can be obtained from the instant results with appropriate choice of various parameters as was done in [27].

In general, wave number and hence the phase velocity of the waves is complex quantity, therefore the waves are attenuated in space. If we write

$$c^{-1} = v^{-1} + \mathrm{i}\omega^{-1} Q \tag{19}$$

so that $\xi = R + \mathrm{i}Q$, where $R = \frac{\omega}{v}$, v and Q are real. Also the roots of characteristic Eq. (8) are, in general complex, and hence we assume that $m_r = p_r + \mathrm{i}q_r$, so that the exponent in the plane wave solution (11) becomes

$$-R\left\{\tfrac{Q}{R}x\sin\theta + m_r^I z\right\} - \mathrm{i}R\left\{x\sin\theta - m_r^R z - vt\right\} \tag{20}$$

where

$$m_r^R = p_r - q_r Q/R,\ m_r^I = q_r + p_r Q/R. \tag{21}$$

This shows that v is the propagation velocity and Q is the attenuation coefficient of the wave. Upon using representation (19) in secular Eqs. (14)–(18), the values of propagation speed v and attenuation coefficient Q for different modes of wave propagation can be obtained. Since $c' = c/v_P$ is the non-dimensional complex phase velocity, so $v' = v/v_P$ and $Q' = v_P Q$ are the non-dimensional phase speed and attenuation coefficient,

respectively. Here dashes have been omitted for convenience. Eq. (11) can be rewritten as

$$(u, w, \phi, T) = \sum_{r=1}^{4} (1, V_r, W_r, S_r) U_r \exp\{-Qx \sin\theta - \lambda_r^I z\} \exp\{\mathrm{i}[\lambda_r^R z - R(x \sin\theta - Vt)]\} \tag{22}$$

with $\lambda_r = R(m_r^R + im_r^I) = \lambda_r^R + \mathrm{i}\lambda_r^I$ (say). From Eq. (22) it can be obtained that the disturbance direction of Rayleigh wave inclines to the free surface at an angle given by $\theta = \cos^{-1}(m_r^R)$. Moreover, it is apparent that

$$|\lambda_r^R|^2 - |\lambda_r^I|^2 = R^2\{(m_r^R)^2 - (m_r^I)^2\},\ |\lambda_r^R||\lambda_r^I| \cos\delta = \tfrac{1}{2}R^2 m_r^R m_r^I$$

where δ is the angle between the real and imaginary part of complex vector λ_r.

Therefore, the phase plane (the plane vertical to vector λ_r^R) and the amplitude plane (the plane vertical to vector λ_r^I) are not parallel to each other any more as observed in Eq. [27] and hence, the maximum attenuation is not along the direction of wave propagation but along the direction of vector λ_r^I. However, it is slightly getting modified due to the thermal relaxation time here.

4. Specific loss

The specific loss is the ratio of energy (ΔW) dissipated in taking a specimen through a stress cycle, to the elastic energy (W) stored in the specimen when the strain is a maximum. The specific loss is the most direct method of defining internal friction for a material. For a sinusoidal plane wave of small amplitude, Kolsky [31], (p. 106) shows that the specific loss $\Delta W/W$ equals 4π times the absolute value of the imaginary part of ξ to the real part of ξ, i.e.

$$\frac{\Delta W}{W} = 4\pi\left|\frac{\mathrm{Im}(\xi)}{\mathrm{Re}(\xi)}\right|,$$

where ξ is a complex number such that $\mathrm{Im}(\xi) > 0$.

Here

$$\frac{\Delta W}{W} = 4\pi\left|\frac{\mathrm{Im}(\xi)}{\mathrm{Re}(\xi)}\right| = 4\pi\left|\frac{vQ}{\omega}\right|. \tag{23}$$

5. Surface displacements, temperature and electric potential

The amplitudes of displacement, electric potential and temperature at the surface $z = 0$ during Rayleigh wave propagation in case of stress and charge free (open circuit), thermally insulated or isothermal boundary of the half space are given by

$$\begin{aligned} u_S &= UA \exp\{-\mathrm{i}R[x \sin\theta - vt]\},\ w_S = WA\, exp\{-\mathrm{i}R[x \sin\theta - vt]\}, \\ \phi_S &= \Phi A \exp\{-\mathrm{i}R[x \sin\theta - vt]\},\ T_S = \Theta A \exp\{-\mathrm{i}R[x \sin\theta - vt]\}, \end{aligned} \tag{24}$$

where

$$\begin{aligned} A &= U_1 \mathrm{e}^{-Qx \sin\theta}, \\ U &= (G_1 - G_2 + G_3 - G_4)/G_1, \\ W &= (G_1 V_1 - G_2 V_2 + G_3 V_3 - G_4 V_4)/G_1, \\ \Phi &= (G_1 W_1 - G_2 W_2 + G_3 W_3 - G_4 W_4)/G_1, \\ \Theta &= (G_1 S_1 - G_2 S_2 + G_3 S_3 - G_4 S_4)/G_1, \end{aligned} \tag{25}$$

and $[u_S, w_S, \phi_S, T_S]'$ denotes the values of the quantities $[u, w, \phi, T]'$ on the surface at $z = 0$. The expressions for these quantities in case of closed circuit boundary of the half space can be obtained from Eqs. (24) and (25) by replacing G_i with G_i', $i = 1, 2, 3, 4$. Clearly, the temperature change on the boundary $z = 0$ vanishes in light

of the secular Eqs. (14) and (18) in case of isothermal, stress free, open or closed circuit surfaces of the half space. This result is in agreement and consistent with the boundary conditions.

6. Paths of surface particles

We now discuss the motion of the surface ($z = 0$) particles of the modified Rayleigh waves. It is observed that when thermomechanical, piezoelectric and pyroelectric couplings are operative, the amplitude and slowness of the waves are no longer real as can be seen from Eqs. (24). This means that the wave is damped and that phase differences exist between the functions u and w. Therefore on the surface $z = 0$, we have

$$u_S = |U|Ae^{i(\alpha-p)},\ w_S = |W|Ae^{i(\beta-p)}, \tag{26}$$

where $\alpha = \arg(U)$, $\beta = \arg(W)$, $p = R(x \sin\theta - vt)$ and A, U, W are given by Eq. (25). Upon using Euler representation of complex numbers and simplifying, the Eq. (26) provides us (on retaining real parts only)

$$u_S = |U|A\cos(\alpha - p),\ w_S = |W|A\cos(\beta - p). \tag{27}$$

Eliminating $p = R(x \sin\theta - Vt)$ from (27), we get

$$\frac{u_S^2}{|U|^2} + \frac{w_S^2}{|W|^2} - 2\frac{u_S w_S}{|U||W|}\cos(\alpha-\beta) = A^2\sin^2(\alpha-\beta). \tag{28}$$

Because

$$\frac{\cos^2(\alpha-\beta)}{|U|^2|W|^2} - \frac{1}{|U|^2|W|^2} = -\frac{\sin^2(\alpha-\beta)}{|U|^2|W|^2} < 1,$$

therefore the Eq. (28) represents an ellipse with semi-major axis (M), semi-minor axis (N) and eccentricity (e), given by

$$M^2 = |U|^2 + |W|^2 + \left\{\left(|U|^2|W|^2\right)^2 + 4|U|^2|W|^2\cos^2(\alpha-\beta)\right\}^{1/2}\frac{A^2}{2} \tag{29}$$

$$N^2 = |U|^2 + |W|^2 - \left\{(|U|^2 - |W|^2)^2 + 4|U|^2|W|^2\cos^2(\alpha-\beta)\right\}^{1/2}\frac{A^2}{2}, \tag{30}$$

$$e^2 = \frac{2\left\{\left(|U|^2 - |W|^2\right)^2 + 4|U|^2|W|^2\cos^2(\alpha-\beta)\right\}^{1/2}}{|U|^2 + |W|^2 + \left\{\left(|U|^2 - |W|^2\right)^2 + 4|U|^2|W|^2\cos^2(\alpha-\beta)\right\}^{1/2}}. \tag{31}$$

If δ^* is the inclination of the major axis to the wave normal, then

$$\tan(2\delta^*) = \frac{2\sqrt{(\tan^2\theta - 1)|U||W|}\cos(\alpha-\beta) - \tan\theta\left(|U|^2 - |W|^2\right)}{(\tan^2\theta - 1)\left(|U|^2 - |W|^2\right) + 4\tan\theta|U||W|\cos(\alpha-\beta)}. \tag{32}$$

For Rayleigh wave ($\theta = 90^\circ$), we obtain

$$\delta^* = \frac{1}{2}\tan^{-1}\left(\frac{2|U||W|\cos(\alpha-\beta)}{\left(|U|^2 - |W|^2\right)}\right). \tag{33}$$

Thus it follows that the surface particles trace elliptical paths given by the Eq. (28) in vertical planes parallel to the direction of wave propagation. The semi axes depend upon $A = U_1 e^{-Qx\sin\theta}$ and hence increase or decrease exponentially. Clearly the decay of elliptical paths of surface particles depends on θ and attenuation coefficient Q. Since Q has maximum value for $\theta = \cos^{-1}(m_r^I)$, therefore for a given value of x, it is concluded that the particles trace elliptical. However, for $\alpha - \beta = \frac{\pi}{2}$, both M and N have same signs and therefore the surface particles describe elliptical paths in the retrograde fashion in this case. Moreover, the particle paths degenerate into straight lines when $\alpha = \beta$, i.e. when there is no phase difference between the functions u_S and w_S.

7. Numerical results and discussion

The material chosen for the purpose of numerical calculations is (6 mm class) cadmium selenide (CdSe) of hexagonal symmetry, which is transversely isotropic material. The physical data for a single crystal of CdSe material is given as [24]

$$
\begin{aligned}
&c_{11} = 7.41 \times 10^{10}\ \mathrm{N\,m^{-2}},\ c_{12} = 4.52 \times 10^{10}\ \mathrm{N\,m^{-2}},\ c_{13} = 3.93 \times 10^{10}\ \mathrm{N\,m^{-2}},\\
&c_{33} = 8.36 \times 10^{10}\ \mathrm{N\,m^{-2}}, c_{44} = 1.32 \times 10^{10}\ \mathrm{N\,m^{-2}},\ \beta_1 = 0.621 \times 10^{6}\ \mathrm{N\,K^{-1}\,m^{-2}},\\
&\beta_3 = 0.551 \times 10^{6}\ \mathrm{N\,K^{-1}\,m^{-2}},\ e_{13} = -0.160\ \mathrm{Cm^{-2}},\ e_{33} = 0.347\ \mathrm{Cm^{-2}},\\
&e_{51} = -0.138\ \mathrm{Cm^{-2}},\ \in_{11} = 8.26 \times 10^{-11}\ C^2\ \mathrm{N^{-1}\,m^{-2}},\ \in_{33} = 9.03 \times 10^{-11}\ C^2\ \mathrm{N^{-1}\,m^{-2}}\\
&C_e = 260\ \mathrm{J\,kg},\ p_3 = -2.94 \times 10^{-6}\ \mathrm{CK^{-1}\,m^{-2}},\ Yr = 4.48 \times 10^{10}\ \mathrm{Nm^{-2}}\\
&\alpha_r = 4.4 \times 10^{-6}\ \mathrm{K^{-1}},\ \alpha_1 = 3.92 \times 10^{-12}\ \mathrm{CN^{-1}},\ K1 = K3 = 9\ \mathrm{W\,m^{-1}\,K^{-1}}\\
&r = 5504\ \mathrm{Kg\,m^{-3}},\ T_{\mathrm{o}} = 298\ \mathrm{K},\ \omega^* = 2.14 \times 10^{13}\ \mathrm{s^{-1}}.
\end{aligned}
$$

Here the thermal relaxation time t_0 is computed from $t_0 = 3K/\rho C_e c_{11}$ and t_1 can be taken as multiple of t_0, because the thermal relaxation effects are short lived and these are more prominent at high-frequencies where conditions are nearly isothermal one. We have considered the secular Eqs. (14) and (15) corresponding to stress and charge free, isothermal and stress-free electrically shorted isothermal boundaries of the half space respectively, in order to demonstrate the numerical solution. These equations are solved by functional iteration method to obtain the phase velocity, attenuation coefficient and specific loss of energy of Rayleigh waves after finding the roots of characteristic Eq. (8) in the context of generalized (LS, GL) and coupled (CT) theories of thermoelasticity. The complex characteristic Eq. (8), being in general of the form $G(m, s, c) = 0$, can be solved for 'm' with the help of DesCartes algorithm along with irreducible case of Cardano's method, for fixed values of c and s. Here, we take $\theta = 75^\circ$ and 90° as the inclinations of wave normal to z-axis and the former choice is approximately close to $\theta = \cos^{-1}(m_r^R)$. The secular Eqs. (14) and (15) are of the form $F(c, m) = 0$. For known values of m this equation can be solved for the complex phase velocity c. We have used functional iteration method to find real phase velocity (v) and attenuation coefficient (Q) for different values of the real wave number (R) upon using representation (19). Here the sequence of the values of phase velocity has been allowed to iterate sufficient number of iterations to make it converge in order to achieve the desired level of accuracy viz. four decimal places. A FORTRAN program is developed and executed on PENTIUM-IV, IBM processor to simulate various quantities and functions. The computed dispersion curves, attenuation coefficient, specific loss profiles, surface displacements, temperature, electric potential and inclinations of major axis with wave normal are plotted in Figs. 1–12.

The Fig. 1 represents phase velocity profiles of Rayleigh waves in charge free (open circuit), isothermal boundary of the half space. It is observed that phase velocity increases for $0 \leqslant R \leqslant 1$ to attain its maximum value at $R = 1$ and decreases at $1 \leqslant R \leqslant 3$ before it becomes stable and steady for all $R \geqslant 3$. The phase velocity in classical and non classical theories of thermoelasticity is observed to follow the trend $v_{\mathrm{GEN}} < v_{\mathrm{CT}}$ for all values of the wave number in case of isothermal boundary in both the considered directions of propagation. The effect of thermal relaxations on the phase velocity of Rayleigh waves is quite pertinent at small values of the wave number; however, it significantly affected by the anisotropy as compared to thermal relaxation at large wave numbers. Fig. 2 pertains to attenuation coefficient profiles with wave number of the Rayleigh waves in charge free (open circuit) isothermal boundary of the half space. It is observed that, the attenuation coefficient increases and remains dispersive in the range of wave number $0 \leqslant R \leqslant 3$, but it varies linearly for $R \geqslant 3$. This quantity of all values of the wave number follows the trend $Q_{\mathrm{CT}} < Q_{\mathrm{GEN}}$ along with the considered directions of propagation, although the effect of thermal relaxation time is quite small but significant at small wave numbers.

Fig. 3 represents the phase velocity profiles of Rayleigh waves in case of electrically shorted (closed circuit) isothermal boundary of the half space. It is clear that, the phase velocity increases and the variations are sinusoidal approximately in the considered range of wave number. It follows the trend of variations as $v_{\mathrm{CT}} < v_{\mathrm{GEN}}$ at all wave numbers; though the effect of thermal relaxation is quite significant for $R \geqslant 4$ rather

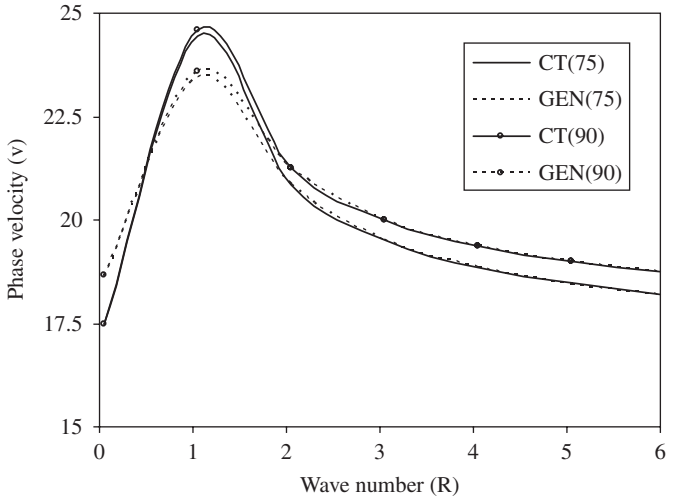

Fig. 1. Variation of phase velocity in open circuit, stress free and isothermal half space with wave number.

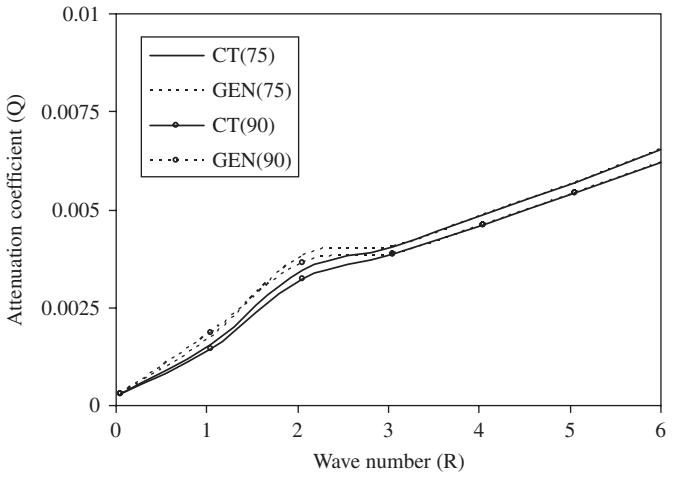

Fig. 2. Variation of attenuation coefficients in open circuit, stress free and isothermal half space with wave number.

than at small values of the wave number. Both thermal relaxation and anisotropy affect the phase velocity at large wave numbers. The attenuation coefficients profiles of Rayleigh waves are presented in Fig. 4 for a closed circuit isothermal boundary of the half space. The attenuation coefficients increases monotonically at all considered values of the wave number. The attenuation follows the trend $Q_{CT} < Q_{GEN}$ in this case for $R \geqslant 0$. However, the attenuation coefficients is quite large at higher wave numbers signifying the fact that as the wave goes deep into the medium it decays exponentially due to the coupling effects of various interacting fields, which is in consistent with the definition of Rayleigh waves. The comparison of Fig. 1 with Fig. 3 and Fig. 2 with Fig. 4 reveal that the thermal relaxation effects on phase velocity and attenuation are quite pertinent and significant at low wave numbers in case of charge free (open circuit) boundary of the half space, where it happens at large wave numbers for electrically shorted (closed circuit) one. The trends of variation among generalized (LS, GL) and coupled (CT) theories of thermoelasticity also get reversed when the electric conditions on the boundaries of the half space are changed from open circuit to closed circuit and vice versa.

Figs. 5 and 6 represent the plots of specific loss factor (SL) with wave number. This gives us the idea about the energy dissipated through a stress cycle to energy stored in the specimen when the strain is maximum. From Fig. 5, it is observed that, the specific loss is maximum at zero wave number which decreases for

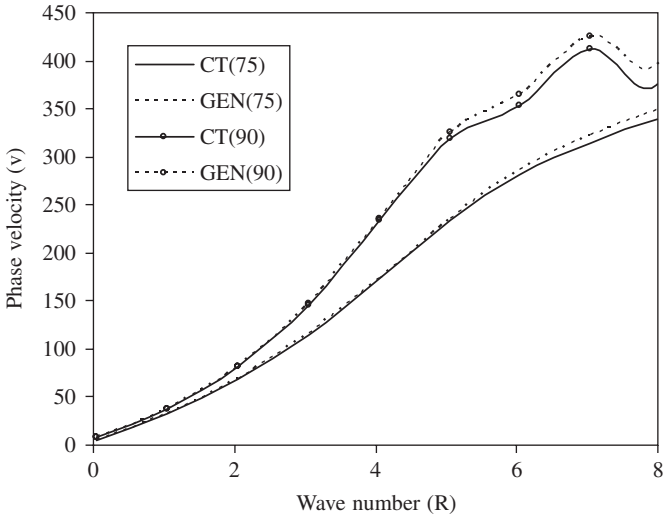

Fig. 3. Variation of phase velocity in closed circuit, stress free and isothermal half space with wave number.

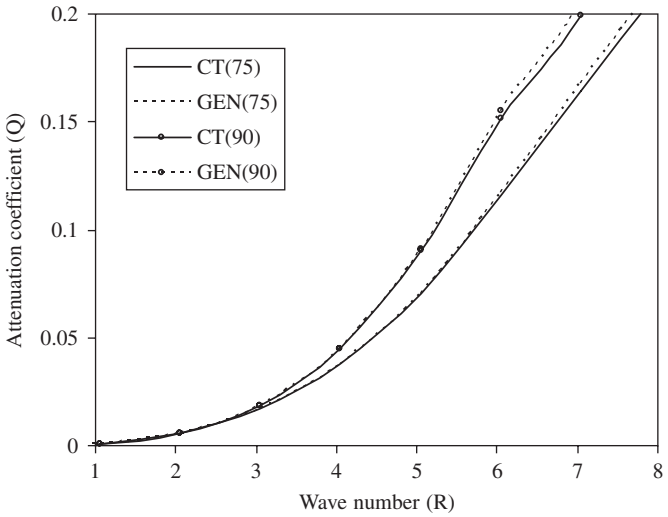

Fig. 4. Variation of attenuation coefficients in closed circuit, stress free and isothermal half space with wave number.

$0 \leqslant R < 3$, and becomes steady and stable for all $R \geqslant 3$ in both the considered directions of wave propagation in stress and charge-free isothermal boundary of the half space. The effect of thermal relaxation is significant in the range $0 \leqslant R \leqslant 3$. It is evident that, the material exhibits more internal friction in generalized theory rather than in coupled theory of thermoelasticity along both the considered direction. Also, the internal friction of considered material is observed to be more along $\theta = 75^\circ$ than along with $\theta = 90^\circ$ in case of coupled (CT) thermoelasticity and it follows reverse trends in generalized thermoelastic solids which is consistent with physical situations too. Fig. 6 reveals that specific loss is quite small at small wave numbers but high at large wave numbers in case of electrically shorted (closed circuit) boundary of the half space. The effect of thermal relaxation in this case is significantly large for $R \geqslant 4$ and negligible elsewhere. However, the material exhibits more internal friction in case of non-classical theories of thermoelasticity as compared to classical one. At all wave numbers specific loss is observed to be quite high along at $\theta = 90^\circ$ rather than along at $\theta = 75^\circ$ in this case. Thus, the specific loss (energy dissipation) is very high when the wave penetrates deep into the medium from the free surface in case of closed circuit boundary of the half space, whereas, it is significantly large when the wave travels in the neighbourhood of the free surface for the case of open circuit boundary. This clearly

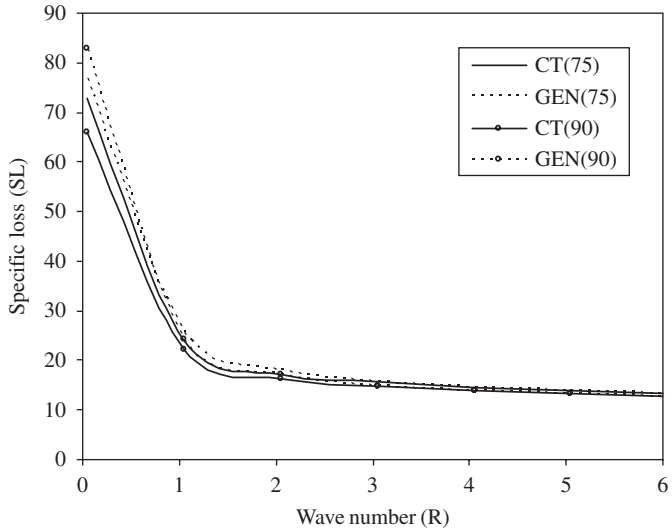

Fig. 5. Variation of specific loss in an open circuit, stress free and isothermal half space with wave number.

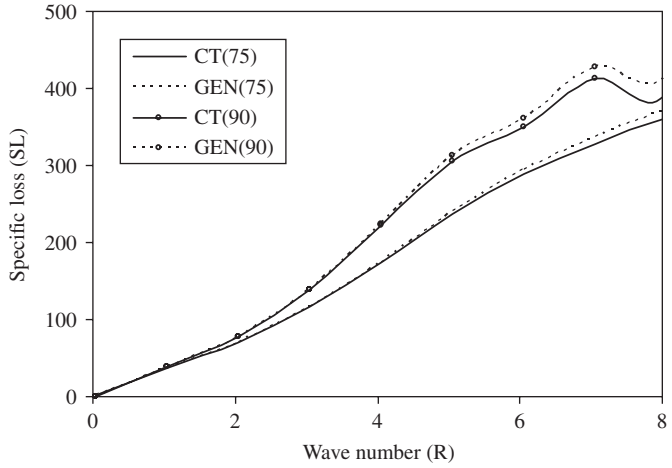

Fig. 6. Variation of specific loss in closed circuit, stress free and isothermal half space with wave number.

depicts the effect of electric polarization in case of open and closed circuit boundary conditions of the piezothermoelastic half space.

Figs. 7 and 8 represent the plots of the inclination (in degrees) of wave normal with major axis of elliptical paths of surface particles during the Rayleigh wave propagation with respect to wave number along $\theta = 75^\circ$ and $\theta = 90^\circ$ in case of phase difference $|\alpha - \beta| = 60^\circ$ for stress and charge free, isothermal and stress free, electrically shorted, isothermal boundaries of the considered half space respectively. From Fig. 7, it is noticed that the inclination of wave normal with major axis decreases from its maximum value ($\delta^* = 19.0712^\circ$ for $\theta = 75^\circ$ and $\delta^* = 18.2092^\circ$ for $\theta = 90^\circ$) at $R = 0$ in the range $0 \leqslant R \leqslant 2$ and remain stable and steady there after for all $R \geqslant 2$. This inclination significantly increases as the wave penetrates deep into the medium and gets affected due to thermal relaxation time with increasing wave number. The affect of anisotropy is also quite significant on this quantity in this case. The examination of Fig. 8 reveals that the magnitude of inclination of wave normal with major axis of elliptical paths of surface particles first decreases in $0 \leqslant R \leqslant 1$ to attain its minimum value ($\delta^* = 11.3712^\circ$ for $\theta = 75^\circ$ and $\delta^* = 12.2350^\circ$ for $\theta = 90^\circ$) at $R = 1$ and then again increases slowly and steadily for all $R \geqslant 1$ to become ultimate stable. The effect of thermal relaxation on this quantity in

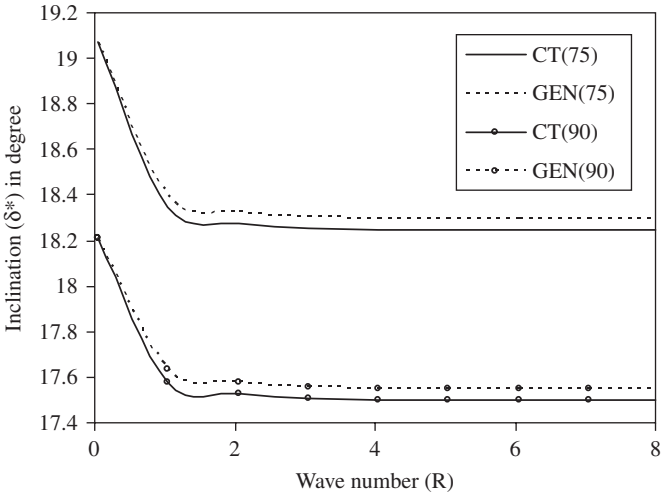

Fig. 7. Inclination of wave normal with major axis in open circuit, stress free and isothermal half space with wave number.

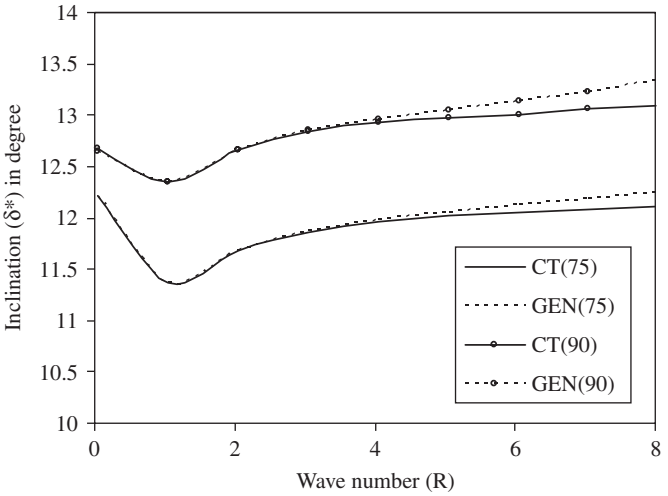

Fig. 8. Inclination of wave normal with major axis in closed circuit, stress free and isothermal half space with wave number.

this case is small but quite pertinent at large values of the wave number. The inclination is significantly affected by the anisotropy affect in this case too. From the comparison of Figs. 7 and 8 it is observed that the inclination of wave normal with major axis of the elliptical paths of surface particles first decreases and then increases as wave number progresses in both the cases of charge free and electrically shorted boundaries of the half space and hence it suffers sign reversals. Thus, it is concluded that the sense of particle paths changes from retrograde to direct at $R = 1$ in both the considered cases of boundary conditions and directions of propagation. This might be attributed to the electrical polarization developments due to the boundary condition and interaction of various coupled fields in the medium. The effect of thermal relaxation time is very small at low values of the wave number as compared to that at higher values in both the cases of open and closed circuit boundary conditions.

The modulus of horizontal ($U_s = |U|A$) and vertical ($W_s = |W|A$) displacements, temperature change ($\Theta_s = |\Theta|A$) and electrical potential (Φ) at the surface in both the cases of open and closed boundary conditions are plotted in Figs. 9–12. It is observed from Fig. 9 that, the horizontal displacement decreases for $0 \leqslant R \leqslant 1$, increases in the wave number range of $1 \leqslant R \leqslant 2.5$ and varies more or less linearly to become stable

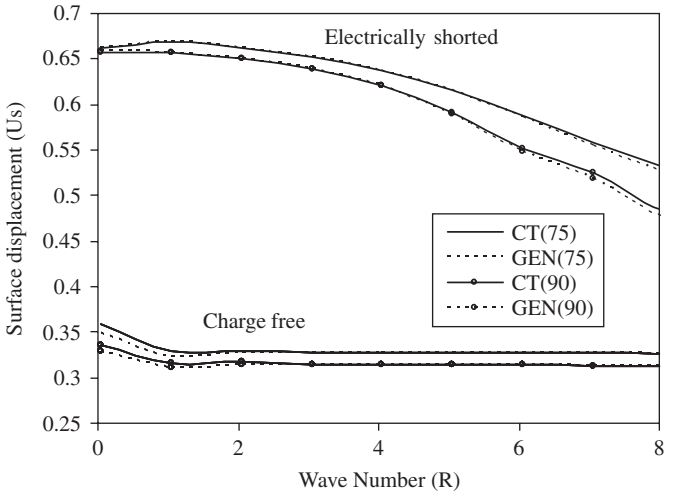

Fig. 9. Variation of horizontal surface displacement in open and closed circuit, stress free and isothermal half space with wave number.

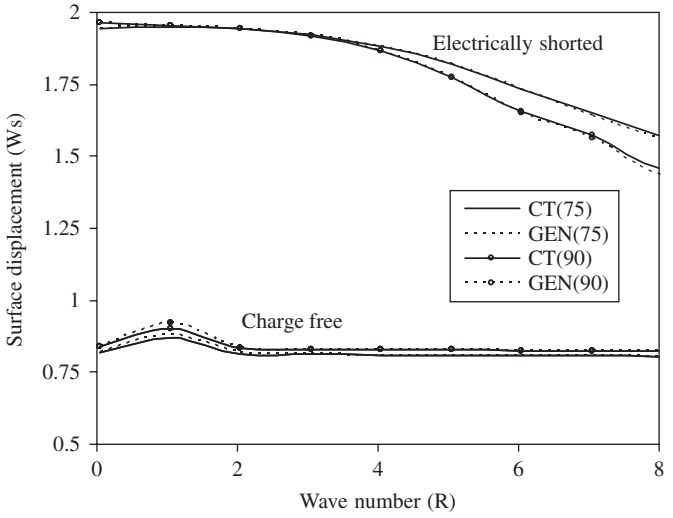

Fig. 10. Variation of vertical surface displacement in open and closed circuit, stress free and isothermal half space with wave number.

afterwards for all in both the considered direction of propagation in case of charge-free boundary of the half space. This quantity in case of electrically shorted half space first increases in $0 \leqslant R \leqslant 1$ and then decreases for $R \geqslant 1$ in both the considered directions. These profiles get affected by the thermal relaxation time at low values of the wave number in the former case and at high wave numbers in the latter one. Fig. 10 reveals that the vertical displacement increases in $0 \leqslant R \leqslant 1$, decreases for $1 \leqslant R \leqslant 2$ and then varies more or less linearly afterwards for $R \geqslant 2$ in case of charge-free conditions and it goes on decreasing after slight increase initially in case of electrically shorted conditions. The phase difference in both the surface displacements is clearly depicted from the profiles given in Figs. 9 and 10. From Fig. 11, it is noted that the electrical potential ($|\Phi|e^{-Q \sin \theta}$) increases for $0 \leqslant R \leqslant 2$ and varies almost linearly after slow variations for all $R \geqslant 2$ in both the considered directions of propagation in an open circuit half space. On the other hand this quantity first increase in $0 \leqslant R \leqslant 1$, decreases for $1 \leqslant R \leqslant 2$ and further decreases after a small increase for all $R \geqslant 2$ in case of closed circuit half space. The electrical potential development is slightly higher when the wave propagates along the surface rather than at positions deep from the surface of the half space in the former case and this trend is reversed in the latter one. The real part of electrical potential amplitude (Φ) is noticed to vanish at the

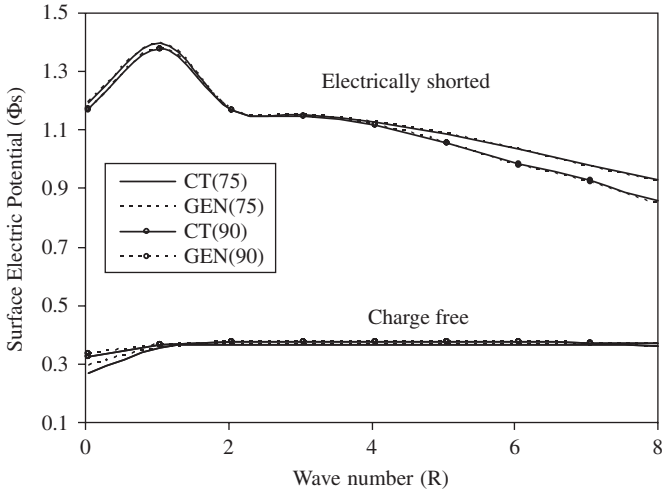

Fig. 11. Variation of surface electric potential in open and closed circuit, stress free and isothermal half space with wave number.

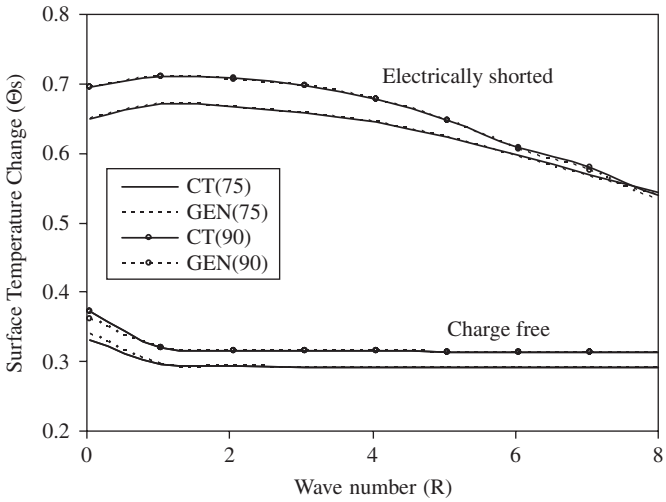

Fig. 12. Variation of surface temperature change in open and closed circuit, stress free and isothermal half space with wave number.

surface in case of electrically shorted boundary of the half space, which is consistent with the physical situation in that case. The temperature change ($|\Theta|e^{-Q \sin \theta}$) profiles in Fig. 12 shows that the temperature change varies almost linearly for $R \geqslant 2$ after suffering a decrease and dispersion in its development in the range $0 \leqslant R \leqslant 2$ of the wave number in case of charge-free boundary. This quantity increases in $0 \leqslant R \leqslant 2$ and decreases for $R \geqslant 2$ in case of electrical shorted boundary of the half space. The effect of thermal relaxation is negligibly small but significant at low wave numbers in open circuit and at large wave numbers in closed circuit half space. Moreover, the real part of temperature change amplitude (Θ) is found to vanish at the surface $z = 0$ in case of considered isothermal boundaries of the half space during Rayleigh wave propagation. This confirms to the boundary condition applied.

Thus, the effect of thermal and electrical boundary conditions on the propagation of Rayleigh waves is quite clear and significant. From the comparison of all the phase velocity and attenuation profiles, it is noticed that while the phase velocity becomes more or less stable and steady with the increase of wave number, the attenuation coefficient increases sharply and indefinitely. This implies that as the wave progresses deep into the semi-space, the coupling between various interacting fields becomes strongly operative which attributes to more attenuation and dissipation of energy thereby exponential decaying of the disturbance. This is quite in

agreement with the occurrence of Rayleigh wave phenomenon. The effect of thermal relaxation is negligible at small wave numbers and quite significant at higher one in case of close circuit half space whereas it gets reversed for open circuit one. This might happen because of resistive phenomenon due to phonon–phonon collision deep into the half space in the former case and close to the surface for latter one in addition to realignments and redistribution of electric charges. The effect of anisotropy is also observed to be significantly high. Similar observation can also be made from the graphs and profiles of various other considered quantities.

8. Conclusions

Thus, in this work the propagation of Rayleigh waves in homogeneous, transversely isotropic, piezothermoelastic half space subjected to (i) stress and charge free, thermally insulated or isothermal; and (ii) stress-free, electrically shorted, thermally insulated or isothermal boundary conditions, has been investigated in the context of generalized theory of thermoelasticity. Secular equations for wave propagation modes in the half space are derived from a coupled system of governing partial differential equations of linear generalized piezothermoelasticity. The analytical expressions for amplitudes of surface displacements, temperature change and electric potential during the Rayleigh wave propagation, have also been obtained. It is observed that the phase velocity profiles along the direction $\theta = 75^\circ$ and 90° in case of stress free thermally insulated or stress free isothermal (both open and closed circuit) surface of the half space are dispersive in character. Because the heat transportation took place through a wave like phenomenon in generalized thermoelasticity instead of diffusive process in coupled thermoelasticity, therefore, a significant effect due to thermal relaxation time is observed on the dispersion curves. The magnitude of phase velocity is observed to be small and that of attenuation as large in generalized piezothermoelastic half space as compared to the coupled one in case of open circuit conditions. This trend gets reversed in case of closed circuit half space for phase velocity but is preserved by attenuation profiles. The value of attenuation coefficient increases with wave number due to the influence of thermal relaxation time and other interacting fields. The numerical computations are found to be in close agreement with analytical results. The specific loss factor and surface particle motion are also discussed. The particle paths on the surface during the motion are found to be elliptical which degenerate in to straight lines when there is no phase difference between the horizontal and vertical components of displacements. The surface particles trace ellipses in retrograde sense when the phase difference between horizontal and vertical displacements is $\frac{\pi}{2}$. However, the sense changes from retrograde to direct one for a phase difference of $\frac{\pi}{3}$ as noticed from numerical results for the considered material. The semi-major and minor axes, eccentricity and inclination of the wave normal with the major axes of the ellipses have also been obtained as analytical expressions. The modulus of complex amplitudes of surface displacements, electrical potential and temperature change are also computed and plotted for illustration purpose.

Acknowledgements

The authors thankfully acknowledge the financial support from the Council of Scientific and Industrial Research (CSIR), New Delhi via project Grants no.25 (0133)/04/EMR-II. The suggestions of the reviewers for the improvement of this work are also thankfully acknowledged.

Appendix

The coefficients a_i, A_i, $i = 1, 2, 3$ in Eq. (8) and $\Delta(m_q)$, $\Delta_i(m_q)$, $i = 1, 2, 3$ in Eq. (9) are defined in [27] and given here for completion purpose.

$$a_1 = \frac{Ps^2 - Jc^2 + \bar{\varepsilon} c_1 c_2 s^2 + \bar{\varepsilon}_\eta \left[(2c_2 e_2 - 2c_3 e_1 + e_1^2 c_1 + 1)s^2 - c^2\right]}{c_1 c_2 + \bar{\varepsilon}_\eta c_2}, \tag{A.1a}$$

$$a_2 = \frac{\bar{\varepsilon}(Ps^2 - Jc^2)s^2 + (s^2 - c^2)(c_2 s^2 - c^2) + \bar{\varepsilon}_\eta \begin{bmatrix} (e_1^2 c_2 + e_2^2 c_2 - 2c_3 e_1 e_2)s^4 \\ -e_1^2 s^2 c^2 + 2e_2 s^2 (s^2 - c^2) \end{bmatrix}}{c_1 c_2 + \bar{\varepsilon}_\eta c_2}, \tag{A.1b}$$

$$a_3 = \frac{s^2(s^2 - c^2)\left[\bar{\varepsilon}(c_2 s^2 - c^2) + \bar{\varepsilon}_\eta e_2^2 s^2\right]}{c_1 c_2 + \bar{\varepsilon}_\eta c_2}, \tag{A.1c}$$

$$A_1 = \frac{\left\{E_1(P' s^2 - J' \bar{c}^2) + \bar{\bar{\varepsilon}} C_1 C_2 s^2 + \bar{\varepsilon}_\eta \left[(2EC_2 \bar{e}_2 - 2E\bar{e}_1 C_3 + \bar{e}_1^2 C_1 + E^2)s^2 - E^2 \bar{c}^2\right]\right\}}{C_1 C_2 E_1 + \bar{\varepsilon}_\eta E^2 C_2}, \tag{A.2a}$$

$$A_2 = \frac{\left\{\begin{matrix} \bar{\bar{\varepsilon}} s^2 (P' s^2 - J' \bar{c}^2)s^2 + E_1(s^2 - \bar{c}^2)(C_2 s^2 - \bar{c}^2) \\ +\bar{\varepsilon}_\eta \left[(\bar{e}_1^2 C_2 + \bar{e}_2^2 C_2 - 2C_3 \bar{e}_1 \bar{e}_2)s^4 + 2E\bar{e}_2(s^2 - \bar{c}^2)s^2 - \bar{e}_1^2 s^2 \bar{c}^2\right] \end{matrix}\right\}}{C_1 C_2 E_1 + \bar{\varepsilon}_\eta E^2 C_2}, \tag{A.2b}$$

$$A_3 = \frac{s^2(s^2 - \bar{c}^2)\left[\bar{\varepsilon}_\eta \bar{e}_2^2 s^2 + \bar{\bar{\varepsilon}}(C_2 s^2 - \bar{c}^2)\right]}{C_1 C_2 E_1 + \bar{\varepsilon}_\eta E^2 C_2}, \tag{A.2c}$$

$$\Delta(m_q) = \tau_1 c s \varepsilon_p \left\{ \begin{matrix} \left[c_3(\bar{\beta}\eta_3 - p) + (\bar{\beta} + pc_1)e_1 - c_1\eta_3 - 1\right] m_q^4 \\ \left[\left(\left\{\begin{matrix} c_3(\bar{\varepsilon}\bar{\beta}\eta_3 - pe_2) + e_1(pc_2 + \bar{\beta}e_2) - 2e_2 \\ -\eta_3(\bar{\varepsilon}c_1 + c_2) \end{matrix}\right\} s^2 \right) - (pe_1 - \eta_3)c^2 \right] m_q^2 \\ -s^2\left[(\bar{\varepsilon}\eta_3 c_2 + e_2^2)s^2 - \bar{\varepsilon}\eta_3 c^2\right] \end{matrix} \right\}, \tag{A.3a}$$

$$\Delta_1(m_q) = -\tau_1 c \varepsilon_P m_q \left\{ \begin{matrix} c_2(\bar{\beta}\eta_3 - p)m_q^4 + \\ \left\{\left[\begin{matrix} \bar{\beta}\eta_3(\bar{\varepsilon}c_2 + 1) + e_1^2\bar{\beta} - p(1 + c_2 e_2 - c_3 e_1) \\ -(\eta_3 c_3 + e_1) \end{matrix}\right] s^2 - (\bar{\beta}\eta_3 - p)c^2 \right\} m_q^2 \\ +s^2\left[(s^2 - c^2)(\bar{\beta}\eta_3\bar{\varepsilon} - pe_2) - (c_3\eta_3\bar{\varepsilon} + e_1 e_2)s^2\right] \end{matrix} \right\}, \tag{A.3b}$$

$$\Delta_2(m_q) = -\tau_1 c m_q \left\{ \begin{matrix} (pc_1 + \bar{\beta})c_2 m_q^4 + \left[\begin{matrix} p(Ps^2 - Jc^2) + \bar{\beta}(s^2 - c^2) \\ +(e_1 c_1 - c_3 + \bar{\beta}e_2 c_2 - \bar{\beta}c_3 e_1)s^2 \end{matrix}\right] m_q^2 \\ +(s^2 - c^2)\left[(pc_2 + \bar{\beta}e_2)s^2 - pc^2\right] \\ +(e_1 c_2 - c_3 e_2)s^4 - e_1 c^2 s^2 \end{matrix} \right\}, \tag{A.3c}$$

$$\Delta_3(m_q) = \in_P \left\{ \begin{matrix} c_2(1 + \eta_3 c_1)m_q^6 + \left[\begin{matrix} -\left\{c_3(c_3\eta_3 + e_1) + e_1(c_3 - c_1 e_1)\right\}s^2 + (\eta_3 c_1 + 1)(s^2 - c^2) \\ +c_2\left\{(c_1\bar{\varepsilon}\eta_3 + c_2\eta_3 + 2e_2)s^2 - \eta_3 c^2\right\} \end{matrix}\right] m_q^4 \\ \left[\begin{matrix} -\left\{c_3(c_3\bar{\varepsilon}\eta_3 + e_1 e_2) + e_1(c_2 e_1 - c_3 e_2)\right\}s^4 + c_2 s^2\left\{\bar{\varepsilon}\eta_3(c_2 s^2 - c^2) + e_2^2 s^2\right\} \\ +(s^2 - c^2)\left\{(c_1\bar{\varepsilon}\eta_3 + c_2\eta_3 + 2e_2)s^2 - \eta_3 c^2\right\} - e_1^2 c^2 s^2 \end{matrix}\right] m_q^2 \\ +(s^2 - c^2)s^2\left\{\bar{\varepsilon}\eta_3(c_2 s^2 - c^2) + e_2^2 s^2\right\} \end{matrix} \right\}, \tag{A.3d}$$

where

$$C_1 = \frac{\left(c_1 - (\varepsilon\bar{\beta}^2\tau_0'\tau_1 \mathrm{i}\omega/\tau_0)\right)}{F'},\ C_2 = \frac{c_2}{F'},\ C_3 = \frac{c_3 - \varepsilon\bar{\beta}\tau_0'\tau_1 \mathrm{i}\omega/\tau_0}{F'},\ \bar{e}_1 = \frac{\left(e_1 + (\varepsilon\varepsilon\tau_0'\tau_1 \mathrm{i}\omega p/\tau_0)\right)}{F'}, \tag{A.4a}$$

$$E=\frac{\left(1+(\varepsilon p\bar{\beta}\tau_0'\tau_1 \mathrm{i}\omega/\tau_0)\right)}{F'},\ \bar{\bar{\varepsilon}}=\frac{\bar{\varepsilon}}{F'},\ E_1=\frac{\left(1+(\varepsilon p^2\tau_0'\tau_1 \mathrm{i}\omega/\eta_3\tau_0)\right)}{F'},\ \bar{c}^2=\frac{c^2}{F'},\ \bar{e}_2=\frac{e_2}{F'},$$
$$F=\frac{\left(1-\varepsilon(\tau_0'\tau_1/\tau_0)i\omega\right)^3 C_2(C_1E_1+\bar{\varepsilon}_\eta E^2)}{C_2(C_1+\bar{\varepsilon}_\eta)},\ F'=1-\frac{\varepsilon\tau_0'\tau_1 i\omega}{\tau_0},\ \bar{\varepsilon}=\frac{\varepsilon}{1+\varepsilon}, \tag{A.4b}$$

$$P=c_1+c_2^2-c_3^2,\ J=c_1+c_2,\ P'=C_1+C_2^2-C_3^2,\ J'=C_1+C_2,$$
$$\tau_0=t_0+\mathrm{i}\omega^{-1},\ \tau_1=t_1\delta_{2k}+\mathrm{i}\omega^{-1},\ \tau_0'=t_0\delta_{1k}+\mathrm{i}\omega^{-1}. \tag{A.4c}$$

References

[1] J. Curie, P. Curie, Development par compression de l'etricite polaire das les cristaux hemledres a faces inclines, Bulletin No. 4 de la Societee Minearalogique de France, **3** (1880).

[2] T.Y. Chen, Further correspondences between plane piezoelectricity and generalized plane strain in elasticity, *Proceedings of Royal Society of London A* 454 (1971) 873–884.

[3] S.I. Chizhikov, N.G. Sorokin, V.S. Petrakov, The elastoeletric effect in the non-centrosymmetric crystal, in: G.W. Taylor, et al. (Eds.), *Piezoelectricity*, Gordon & Breach Science Publishers, New York, 1985, pp. 75–91.

[4] J.H. He, Coupled variational principles of piezoelectricity, *International Journal of Engineering Science* 39 (2001) 323–341.

[5] G.A. Maugin, *The Mechanical Behaviour of Electromagnetic Solid Continua*, North-Holland, Amsterdam, 1984.

[6] G.A. Maugin, *Continuum Mechanics of Electromagnetic Solid*, North-Holland, Amsterdam, 1988.

[7] R.D. Mindlin, On the equations of motion of piezoelectric crystals, in: *Problems of Continuum Mechanics*, SIAM, Philadelphia, N.I. Muskelishvili's Birthday 70 (1961) 282–290.

[8] R.D. Mindlin, *Equation of High Frequency Vibrations of Thermo-piezoelectric, Crystal Plates, Interactions in Elastic Solids*, Springer, Wien, 1979.

[9] W. Nowacki, Some general theorems of thermo-piezoelectricity, *Journal of Thermal Stresses* 1 (1978) 171–182.

[10] W. Nowacki, Foundations of linear piezoelectricity, in: H. Parkus (Ed.), *Electromagnetic Interactions in Elastic Solids*, Springer, Wien, 1979 (Chapter 1).

[11] W. Nowacki, Mathematical models of phenomenological piezoelectricity, in: *New problems in Mechanics of Continua*, University of Waterloo Press, Ontario, 1983, pp. 29–49.

[12] D.S. Chandrasekhariah, A temperature rate dependent theory of piezoelectricity, *Journal of Thermal Stresses* 7 (1984) 293–306.

[13] D.S. Chandrasekhariah, A generalized linear thermoelasticity theory of piezoelectric media, *Acta Mechanica* 71 (1988) 39–49.

[14] A.K. Pal, Surface waves in a thermo-piezoelectric medium of monoclinic symmetry, Czechoslovak, *Journal of Physics* 29 (1979) 1271–1281.

[15] H.S. Paul, K. Ranganatham, Free vibrations of a pyroelectric layer of hexagonal (6 mm) class, *Journal of the Acoustical Society of America* 78 (1985) 395–397.

[16] H.S. Paul, G.V. Raman, Wave propagation in a hollow pyroelectric circular cylinder of crystal class-6 mm, *Acta Mechanica* 87 (1991) 37–46.

[17] H.S. Paul, G.V. Raman, Vibrations of pyroelectric plates, *Journal of the Acoustical Society of America* 90 (1991) 1729–1732.

[18] F. Ashida, T.R. Tauchert, N. Noda, Response of a piezoelectric plate of a crystal class (6 mm) subject to axi-symmetric heating, *International Journal of Engineering Science* 31 (1993) 373–384.

[19] E. Radzikowska, Thermo piezoelectricity equation of plates, *Bulletin Academy Polonaise des Science, Serial Science and Technology* 29 (1981) 195–203.

[20] F. Ashida, T.R. Tauchert, An inverse problem for determination of transient surface from piezoelectric sensor measurement, *ASME Journal of Applied Mechanics* 65 (1998) 367–373.

[21] J.S. Yang, R.C. Batra, Free vibrations of a linear thermo-piezoelectric body, *Journal of Thermal Stresses* 18 (1995) 247–262.

[22] H.W. Lord, Y. Shulman, The generalized dynamical theory of thermoelasticity, *Journal of Mechanics Physics, Solids* 15 (1967) 299–309.

[23] A.E. Green, K.A. Lindsay, Thermoelasticity, *Journal of Elasticity* 2 (1972) 1–7.

[24] J.N. Sharma, M. Kumar, Plane harmonic waves in piezo-thermoelastic materials, *Indian Journal of Engineering and Material Science* 7 (2000) 434–442.

[25] J.N. Sharma, M. Pal, Propagation of Lamb waves in a transversely isotropic piezothermoelastic plate, *Journal of Sound and Vibration* 270 (2004) 587–610.

[26] J.N. Sharma, M. Pal, D. Chand, Thermoelastic Lamb waves in electrically shorted transversely isotropic piezoelectric plate, *Journal of Thermal Stresses* 27 (2004) 33–58.

[27] J.N. Sharma, M. Pal, D. Chand, Propagation characteristics of Rayleigh waves in transversely isotropic piezothermoelastic materials, *Journal of Sound and Vibration* 284 (2005) 227–248.

[28] J.N. Sharma, M. Pal, D. Chand, Three dimensional vibrational analysis of a piezothermoelastic cylindrical panel, *International Journal of Engineering Science* 42 (2004) 1655–1673.
[29] J.N. Sharma, V. Walia, Straight and circular crested waves in generalized piezothermoelastic materials, *Journal of Thermal Stresses* 29 (2006) 529–551.
[30] J.D. Achenbach, The thermoelasticity of laser-based ultrasonic, *Journal of Thermal Stresses* 28 (2005) 713–728.
[31] H. Kolsky, *Stress Waves in Solids*, Clarendon Press, Oxford, 1935 Dover Press New York (1963).